particles

MDPI

Article

Spin Physics at PHENIX †

Devon Loomis on behalf of the PHENIX Collaboration

Department of Physics, University of Michigan, Ann Arbor, MI 48109-1040, USA; dloom@umich.edu

† This paper is based on the talk at the 13th International Conference on New Frontiers in Physics (ICNFP 2024), Crete, Greece, 26 August–4 September 2024.

Abstract: Situated at the Relativistic Heavy Ion Collider (RHIC) at Brookhaven National Laboratory, the PHENIX experiment has for almost two decades been at the forefront of investigations into spin structure and dynamics in high-energy nuclear physics. Although decommissioned in 2016, the PHENIX collaboration has released a number of new results over the past several years that continue to inform the field. Recent longitudinal spin measurements uncover the role of gluon and sea quark polarization in the proton. Transverse spin measurements probe the transverse momentum-dependent (TMD) distributions and higher-twist multiparton correlators that are needed to fully explain partonic dynamics in the initial and final state. Additionally, the effects of heavy ions on spin have been studied by comparing transverse spin measurements between p+p and p+A collisions. These recent results and their wider implications are presented.

Keywords: PHENIX; spin physics; gluon helicity; sea quark polarization; multiparton correlators

1. Introduction

As the lightest stable bound state in quantum chromodynamics (QCD), the proton serves as an excellent laboratory for investigating quarks and gluons—together known as partons—and the hadronic bound states that they form. By polarizing the proton, additional spin degrees of freedom become available as a tool to further test this interplay between the partons and hadrons. The research field of nuclear spin physics takes advantage of these tools to explore fundamental questions related to the structure and dynamics of QCD and its bound states. One of the central questions in the field is how the spin of the proton arises from its fundamental constituents. The proton spin can be decomposed into contributions from the quark polarization, the gluon polarization, and their respective orbital angular momentum [1],

$$\frac{1}{2} = \frac{1}{2}\sum \Delta q + \Delta g + L_q + L_g \,, \tag{1}$$

where the quark and gluon polarization contributions can be written as the integrals of their respective helicity distributions over Bjorken-x, $\Delta q = \int_0^1 \Delta q(x)dx$ and $\Delta g = \int_0^1 \Delta g(x)dx$. The quark polarization sum runs over the valence and sea quarks, $\sum \Delta q = \sum\left(\Delta u + \Delta \bar{u} + \Delta d + \Delta \bar{d} + \Delta s + \Delta \bar{s}\right)$. These helicity distributions describe the difference in longitudinally polarized proton densities with partons of positive versus negative helicity. Measurements in polarized deep-inelastic scattering (DIS) [2–6] and semi-inclusive deep-inelastic scattering (SIDIS) [7,8] have helped constrain the contribution from the quark helicity to ∼30% of the total proton spin. While polarized DIS can access Δg at next-to-leading order (NLO) through photon–gluon fusion, polarized proton collisions at RHIC offer improved sensitivity to the gluon helicity through leading-order (LO) quark–gluon

check for updates

Academic Editors: Larissa Bravina, Sonia Kabana and Armen Sedrakian

Received: 31 December 2024
Revised: 25 January 2025
Accepted: 8 February 2025
Published: 10 February 2025

Citation: Loomis, D., on behalf of the PHENIX Collaboration. Spin Physics at PHENIX. *Particles* **2025**, *8*, 14. https://doi.org/10.3390/particles8010014

Copyright: © 2025 by the author. Licensee MDPI, Basel, Switzerland. This article is an open access article distributed under the terms and conditions of the Creative Commons Attribution (CC BY) license (https://creativecommons.org/licenses/by/4.0/).

and gluon–gluon interactions. Measurements sensitive to Δg from PHENIX [9–11] and its counterpart experiment STAR [12–14] led to the first evidence of significant nonzero gluon polarization at $x > 0.05$ [15,16]. Recent measurements at RHIC, with both larger luminosity datasets and higher collision center-of-mass energies, are focused on pushing towards smaller uncertainties and exploring the small-x region of the gluon helicity.

Helicity distributions are just one of a set of distributions that generalize the standard unpolarized parton distribution functions (PDFs) to account for the polarizations of both the partons and the proton. These PDFs can in general depend on the partonic transverse momentum k_T and are therefore called Transverse Momentum-Dependent (TMD) PDFs. In the case of the unpolarized PDFs, the helicity distributions, and the transversity distributions (the analogue of helicity distributions for transversely polarized protons), the k_T dependence integrates out and the distributions describe correlations between the spin of the parton and the spin of the proton. The remaining TMDs explicitly depend on k_T and encode correlations between the partonic momentum and the proton spin. A set of corresponding TMD fragmentation functions (FFs) exists in the final state, describing spin–momentum correlations between the struck parton and the hadron that it fragments into. The two most prominent examples of TMDs in spin physics are the Sivers TMD PDF [17,18], which correlates the transverse momentum of an initial-state parton with the transverse spin of the proton, and the Collins TMD FF [19], which correlates the transverse spin of a struck quark with preferential directions of the fragmenting hadrons. Both of these functions have been measured to be nonzero through azimuthal asymmetries observed in particle production from SIDIS [20–26] and electron-positron annihilation [27].

Experimental access to TMDs relies on the availability of two scales, scale Q to separate out the partonic-level hard scattering, and soft scale $k_T \ll Q$ that is sensitive to the nonperturbative partonic transverse momentum. In measurements with only one accessible scale (the hard scale Q), such as high p_T production of inclusive particles from hadronic collisions, it is more natural to describe the PDFs and FFs in their collinear limit. In this framework, one encounters correlation terms at $n = 3$ in the $1/Q^{n-2}$ factorization expansion of the cross-section (where n is the twist). These twist-3 correlation functions describe quantum interference between the scattering amplitudes of a single active parton and a composite parton state with an extra gluon. They can describe multiparton quark–gluon [28,29] or trigluon [30,31] correlations. When convoluted together with the standard PDFs and FFs, the twist-3 correlators can generate azimuthal asymmetries in particle production from $p^{\uparrow} + p$ collisions that are known as transverse single spin asymmetries,

$$\begin{aligned} A_N \propto & \sum_{a,b,c} \phi^{(3)}_{a/A}(x_1, x_2, \vec{s}_\perp) \otimes \phi_{b/B}(x') \otimes \hat{\sigma} \otimes D_{c\to C}(z) \\ & + \sum_{a,b,c} \delta q_{a/A}(x, \vec{s}_\perp) \otimes \phi^{(3)}_{b/B}(x'_1, x'_2) \otimes \hat{\sigma}' \otimes D_{c\to C}(z) \\ & + \sum_{a,b,c} \delta q_{a/A}(x, \vec{s}_\perp) \otimes \phi_{b/B}(x') \otimes \hat{\sigma}'' \otimes D^{(3)}_{c\to C}(z_1, z_2) \,, \end{aligned} \tag{2}$$

where Superscript (3) terms represent the twist-3 correlators and all other terms are at the leading twist-2. From Equation (2), the asymmetry can originate from an initial-state "Sivers-like" twist-3 correlator, $\phi^{(3)}$, coupled with a leading-twist fragmentation function, D, or a final-state "Collins-like" correlator, $D^{(3)}$, coupled with a leading-twist transversity distribution, δq. The twist-3 functions can be related to the k_T moments of the TMD PDFs and FFs. Observables at PHENIX are chosen for their sensitivity to specific twist-3 correlators and, by extension, specific TMDs. As an example, the direct photon A_N provides a considerably powerful constraint on the twist-3 quark–gluon and trigluon correlators because the clean final state minimizes any twist-3 contribution from fragmentation.

2. Experiment

The Relativistic Heavy Ion Collider (RHIC) provides the spin physics community with the unique opportunity to study spin observables from high-energy polarized proton collisions. The collection of polarized physics runs at RHIC relevant for PHENIX data taking are outlined in Table 1.

Table 1. PHENIX polarized physics data taking runs.

Year	System	$\sqrt{s}$ (GeV)	Polarization Direction	Recorded Luminosity [pb^{-1}]
2006	p + p	62.4	transverse	0.02
			longitudinal	0.08
		200	transverse	2.7
			longitudinal	7.5
2008	p + p	200	transverse	5.2
2009	p + p	200	longitudinal	16
		500		14
2011	p + p	500	longitudinal	18
2012	p + p	200	transverse	9.7
		510	longitudinal	32
2013	p + p	510	longitudinal	155
2015	p + p	200	transverse	60
	p + Au			1.27
	p + Al			3.97

Located at the 8 o'clock interaction point on the RHIC ring, the PHENIX detector, shown in Figure 1, was built for the high-resolution measurement of hadrons, photons, electrons, and muons. Two central arms, each with $\Delta\phi = \pi/2$ azimuthal and $|\eta| < 0.35$ pseudorapidity coverage, were outfitted with high granularity electromagnetic calorimeters, drift and pad chambers for track reconstruction, a Ring-Imaging Cherenkov Detector for e/π discrimination, and a silicon vertex detector for primary and secondary vertex reconstruction. Muon arms with full azimuthal coverage at intermediate pseudorapidity, $1.2 < |\eta| < 2.4$, measured charged particle momentum and provided muon and charged hadron identification. At forward rapidity, the Muon Piston Calorimeters were full azimuth electromagnetic calorimeters from $3.1 < |\eta| < 3.8$, and the beam–beam counter was a global event characterization detector responsible for luminosity counting and providing a minimum bias trigger. Upstream of the interaction region in the RHIC tunnel, the zero-degree calorimeters provided hadronic calorimetry intended for far-forward neutron detection at $|\eta| > 6.8$. A thorough description of the PHENIX detector and its capabilities can be found in the detector overview [32].

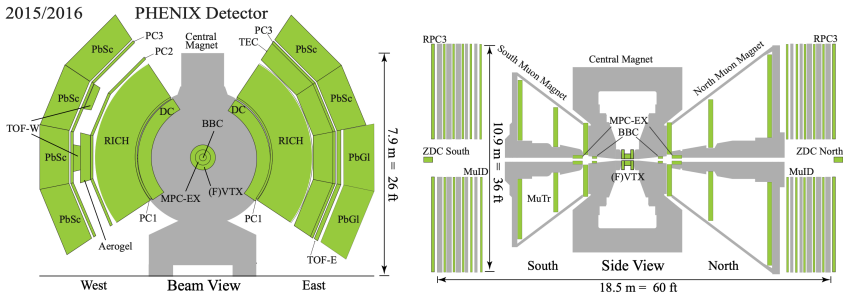


Figure 1. (**Left**): The PHENIX detector from the point of view of the beam. (**Right**): A cross-sectional view of the PHENIX detector when viewed from the side.

3. Results

3.1. Longitudinal Spin

At RHIC energies, hard scattering occurs mostly through quark–gluon and gluon–gluon interactions. As such, PHENIX observables from longitudinally polarized proton collisions provide unparalleled access to the gluon helicity distribution through measurements of their longitudinal double spin asymmetries,

$$A_{LL} = \frac{\sigma^{++} - \sigma^{+-}}{\sigma^{++} + \sigma^{+-}} \propto \frac{\Delta\sigma}{\sigma} \, . \tag{3}$$

Here, $\sigma^{++}(\sigma^{+-})$ denotes the cross-section from collisions of protons with like (opposite) helicities and $\Delta\sigma(\sigma)$ is the helicity (unpolarized) cross-section. The helicity cross-section is the convolution of the partonic helicity distributions with the partonic cross-section,

$$\Delta\sigma = \sum \Delta f_{a/A} \otimes \Delta f_{b/B} \otimes \Delta\sigma_{ab} \, , \tag{4}$$

for partons a, b and hadrons A, B, where we neglected any fragmentation effects. In most cases at RHIC, at least one of the parton helicity distributions is $\Delta g(x)$.

3.1.1. Direct Photon A_{LL}

The cleanest measurement of the gluon helicity is the longitudinal double spin asymmetry of direct photons. The production of direct photons comes predominantly from quark–gluon Compton scattering, leading to minimal contributions from fragmentation in the final state. Additionally, the A_{LL} from direct photons has a linear dependence in $\Delta g(x)$ and is therefore sensitive to its sign.

This is particularly relevant considering the recent study [33] that found consistent positive and negative solutions for the gluon helicity after relaxing a positivity constraint. A response paper [34] argues that the relaxing of such a constraint leads to unphysical predictions. The direct photon A_{LL} can serve as an experimental arbiter to this question. In Run 13, PHENIX measured the direct photon A_{LL} at $\sqrt{s} = 510$ GeV, the first measurement of its kind [35]. Figure 2 shows the direct photon A_{LL}, which favors the positive solution of Δg at 2.8σ.

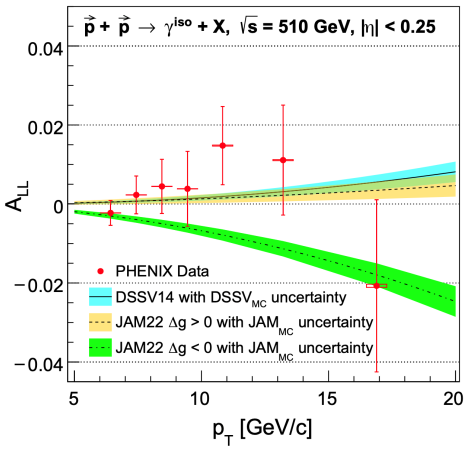


Figure 2. The direct photon longitudinal double spin asymmetry [35] compared to phenomenological predictions from DSSV [36] and JAM [37] where JAM considers the possiblity of either $\Delta g > 0$ or $\Delta g < 0$.

3.1.2. Pion A_{LL}

While the first evidence of nonzero gluon polarization was discovered at high x, the low-x behavior of the gluon helicity is still largely unconstrained due to a lack of

experimental data. In order to probe the $x < 0.05$ region of $\Delta g(x)$, PHENIX measured the $\pi^{\pm}$ A_{LL} at the increased center of mass energy of $\sqrt{s} = 510$ GeV [38] to go along with a previous measurement from $\sqrt{s} = 200$ GeV [39]. This improved the downward reach in x_T by about a factor of two (Figure 3).

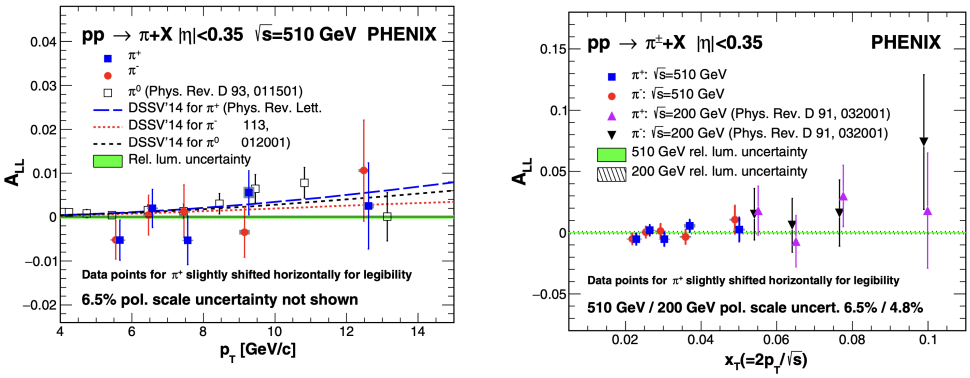


Figure 3. (**Left**): The p_T dependent A_{LL} for pions at $\sqrt{s} = 510$ GeV [38] compared to predictions made using the global DSSV helicity fits [15]. (**Right**): The x_T dependent A_{LL} for pions at $\sqrt{s} = 510$ GeV [38] and $\sqrt{s} = 200$ GeV [39].

3.1.3. W Boson A_L

In addition to helping set constraints on the gluon polarization in the proton, PHENIX investigated the helicity of sea quarks through the measurement of the longitudinal single spin asymmetry of the W boson. The maximally parity-violating electroweak process $u_L\bar{d}_R \to W^+$, $\bar{u}_R d_L \to W^-$ fixes the handedness of the quarks and antiquarks such that reversing the polarization direction of the proton flips the corresponding helicities of the quarks. The longitudinal single spin asymmetry is thus proportional to a mixture of the helicities and unpolarized PDFs of the quarks and anti-quarks,

$$A_L^{W^-} = \frac{\sigma^+ - \sigma^-}{\sigma^+ + \sigma^-} \approx \frac{\Delta\bar{u}(x_1)d(x_2) - \Delta d(x_1)\bar{u}(x_2)}{\bar{u}(x_1)d(x_2) + d(x_1)\bar{u}(x_2)}. \quad (5)$$

$W^{\pm}$ are detected through their leptonic decay modes such that the charge and kinematics of the decay lepton allow for the flavor separation of the sea quarks. This means that this measurement is sensitive to the polarized sea quark asymmetry $\Delta\bar{u} - \Delta\bar{d}$. Results of the W boson A_L from PHENIX [40,41] and STAR [42] are shown in Figure 4, hinting at a positive polarized sea asymmetry. An additional high-precision W A_L from STAR [43] was included in an update to the NNPDFpol1.1 global fit [16], which indicated for the first time the clear positive signature of the asymmetry.

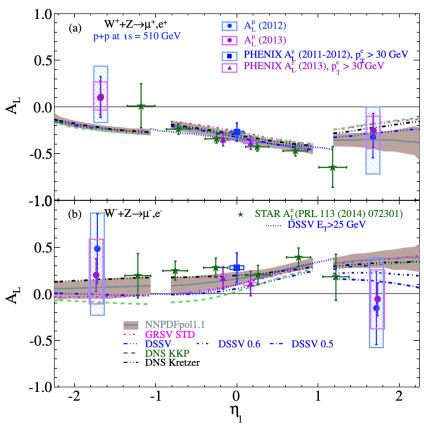


Figure 4. The PHENIX [40,41] and STAR [42] longitudinal single spin asymmetries for (**a**) W^+ bosons and (**b**) W^- bosons.

3.2. Transverse Spin

In transversely polarized $p^{\uparrow} + p$ collisions, particle production is to first-order azimuthally dependent on a cosine modulation. The magnitude of this modulation is the same transverse single spin asymmetry A_N of Equation (2), and it is measured experimentally by

$$A_N \cos\phi = \frac{1}{P} \frac{d\sigma^{\uparrow}(\phi) - d\sigma^{\downarrow}(\phi)}{d\sigma^{\uparrow}(\phi) + d\sigma^{\downarrow}(\phi)}, \tag{6}$$

where P is the beam polarization and $d\sigma^{\uparrow,\downarrow}(\phi)$ are the cross-sections differential in the azimuth for polarized up and polarized down protons, respectively. The goal of the transverse spin physics program at PHENIX is to measure A_N across an array of different final-state particles, which are each uniquely suited to provide constraints on some subset of the twist-3 correlators.

3.2.1. Direct Photon A_N

As stated in Section 1, direct photon observables mitigate any final-state color effects, leaving the direct photon A_N directly sensitive to quark–gluon and trigluon correlators in the initial state only. A recent PHENIX measurement of the midrapidity direct photon A_N at $\sqrt{s} = 200$ GeV [44] is shown in Figure 5 with a comparison to theoretical predictions of the contributions to the asymmetry from the quark–gluon [45] and trigluon correlators [46]. The measurement is consistent with both the model predictions and zero asymmetry but with a 50-time statistical improvement from the previous best measurement at Fermilab E704 [47].

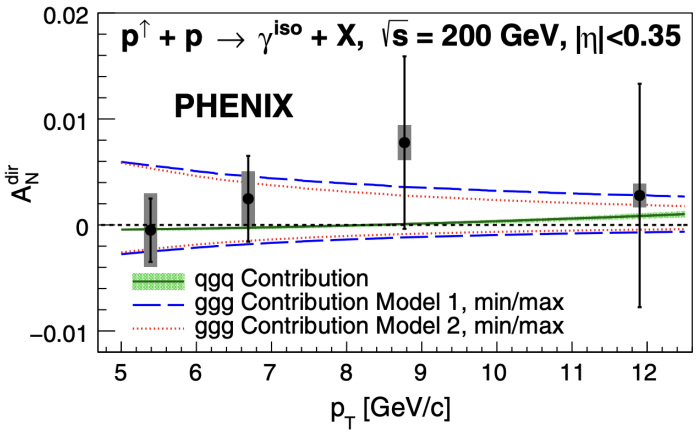


Figure 5. The direct photon transverse single spin asymmetry from PHENIX [44] plotted alongside model predictions of the A_N generated by quark–gluon and trigluon correlators.

3.2.2. Open Heavy Flavor A_N

PHENIX also measured the midrapidity open heavy flavor A_N at $\sqrt{s} = 200$ GeV [48], shown in Figure 6. The open heavy flavor A_N isolates the twist-3 initial-state trigluon correlators because (a) the process is dominated by gluon–gluon fusion and (b) gluons have no transversity within the spin 1/2 proton, hence eliminating any twist-3 effects from the final state. Not much is known of the trigluon functions, so a typical phenomenological strategy is to parameterize them in relation to the much better understood unpolarized gluon PDF [46,49]. Scanning through the parameter space and comparing the predictions to the experimental results enabled this measurement to place the first experimental constraints on these parameters: $\lambda_f, \lambda_d, K_G, K'_G$.

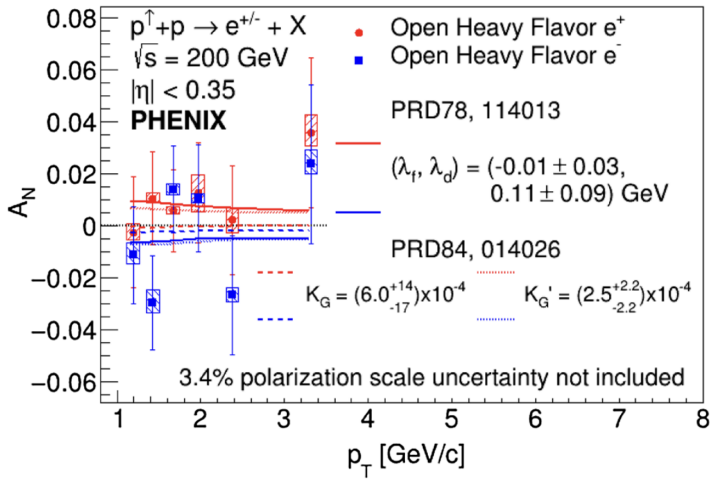


Figure 6. The open heavy flavor $e^{\pm}$ transverse single spin asymmetry from PHENIX [48] compared with theoretical predictions from the trigluon correlators using the best-fit parameters determined by the measurement.

3.2.3. Forward Charged Hadron and η Meson A_N

At forward rapidities, PHENIX recently observed large transverse single spin asymmetries at high Feynman-x (x_F) in charged hadron [50] and preliminary η meson results (Figure 7).

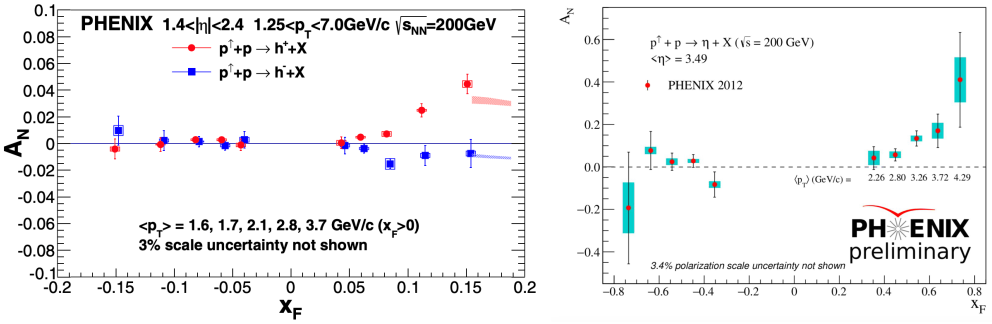


Figure 7. (**Left**): The forward ($1.4 < |\eta| < 2.4$) charged hadron transverse single spin asymmetries at PHENIX [50]. (**Right**): The preliminary forward ($\langle\eta\rangle = 3.49$) transverse single spin asymmetry of the η meson at PHENIX.

These measurements agree with previous findings and have a broader kinematic reach to higher x_F. Forward production of hadrons is dominated by valence quark interactions, suggesting that a significant contribution to the asymmetries must originate from twist-3 quark–gluon correlators in either the initial state, final state, or both. Recent phenomenological studies [51,52] appear to indicate that, at least in the light meson sector, the initial-state twist-3 quark–gluon correlator by itself is insufficient to describe the size of the observed asymmetries and a consistent description between asymmetries in SIDIS and proton–proton collisions relies predominantly on twist-3 fragmentation.

3.2.4. Forward Charged Hadron A_N in $p^{\uparrow} + A$

The forward charged hadron transverse single spin asymmetries were also measured in $p^{\uparrow} + Al$ and $p^{\uparrow} + Au$ [53]. When compared with $p^{\uparrow} + p$, PHENIX observed striking behavior suggesting a nuclear modification of A_N, which looks like $A^{-1/3}$, as shown in Figure 8 (left). A follow-up study measured A_N differentially in x_F with a much larger dataset and confirmed the suppression of the asymmetry as a function of mass number [50].

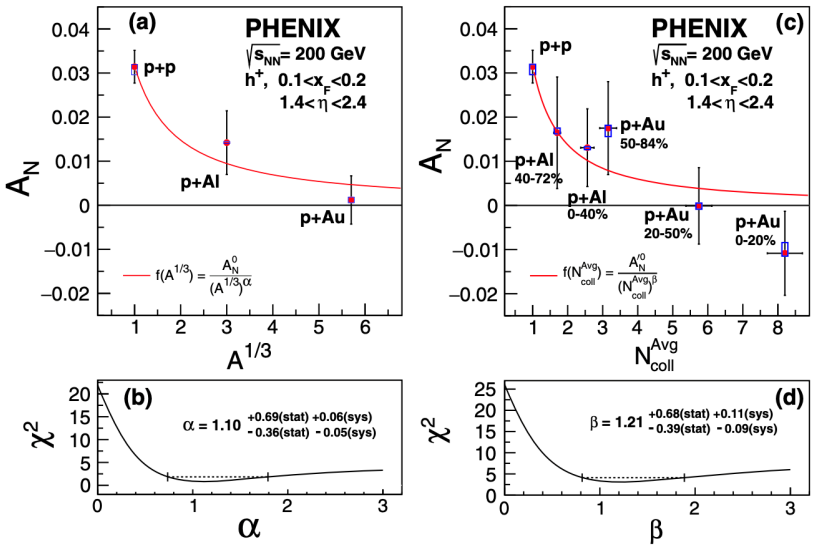


Figure 8. The forward charged hadron transverse single spin asymmetry observed in $p^{\uparrow}+p$, $p^{\uparrow}+Al$, $p^{\uparrow}+Au$ [53] at PHENIX. (**Left**): (**a**) The A_N as a function of mass number $A^{1/3}$. (**b**) The best-fit of the exponent, α where $A_N \sim (A^{1/3})^{\alpha}$. (**Right**): (**c**) The A_N as a function of the number of average nucleon–nucleon collisions, $N_{\text{coll}}^{\text{Avg}}$ calculated using the Glauber model [54]. (**d**) The best-fit of the exponent, β, where $A_N \sim (N_{\text{coll}}^{\text{Avg}})^{\beta}$.

The proper theoretical description of this behavior is still elusive. Some calculations of A_N in $p^{\uparrow}+A$ that account for gluon saturation effects find that such behavior is possible when in the saturation regime, but the PHENIX measurement is well above the saturation scale in the Au nucleus, violating the condition needed for strong nuclear suppression [55]. Multiple scattering between the struck quark and nucleons has been suggested as a mechanism to suppress the azimuthal asymmetries in SIDIS [56]. This argument has yet to be extended theoretically to hadronic collisions, but it may warrant further investigation as the experimental observation of suppression of A_N with respect to the average number of nucleon–nucleon collisions shown in Figure 8 (right) suggests dependence of A_N on the density of the nuclear matter, a variable closely connected to the likelihood of multiple scatters.

3.2.5. Far-Forward Neutron A_N

At far-forward rapidities in PHENIX, the measurement of the nontrivial nuclear dependence of the neutron transverse single spin asymmetry [57] shown in Figure 9 has been the subject of considerable study. In this region, the mechanisms for producing particles are dominated by soft QCD processes, like one-pion exchange and diffractive scattering. While forward neutron yields have been well described using one-pion exchange models, the large negative neutron A_N in $p^{\uparrow}+p$ collisions require a more subtle explanation of interference between the neutron production amplitudes from one-pion exchange and Reggeon exchange [58]. This mechanism, however, could not explain the large dependence and sign change of the asymmetry on the mass number in $p^{\uparrow}+A$ collisions.

The explanation for this initially unexpected behavior is that electromagnetic interactions from ultra-peripheral collisions (UPCs) generate large positive asymmetries that are highly dependent on the mass number [59]. This is reflected in Figure 9 where the ZDC⊗BBC-veto trigger requirement enhances the UPC contribution to A_N while the ZDC⊗BBC-tag trigger requirement enhances the hadronic contribution. More recently, the very forward neutron asymmetries have been measured as a function of p_T and x_F with these separate trigger conditions [60]. Model calculations that include contributions from

one-pion exchange and UPC qualitatively describe the behavior reasonably well, as seen in Figures 10 and 11.

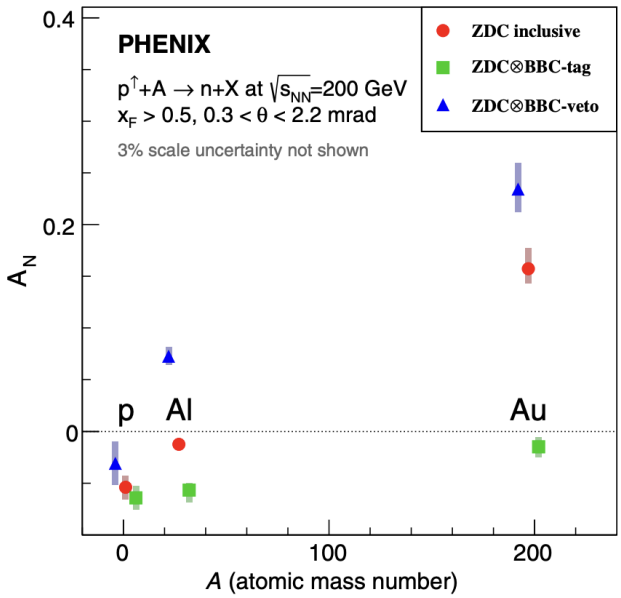


Figure 9. The far-forward neutron transverse single spin asymmetry at PHENIX for $p^{\uparrow} + p$, $p^{\uparrow} + Al$, $p^{\uparrow} + Au$ collisions [57]. The red circles represent inclusive neutrons, the green squares represent a neutron sample with enhanced hadronic contributions, and the blue triangles represent a neutron sample with enhanced electromagnetic (UPC) contributions.

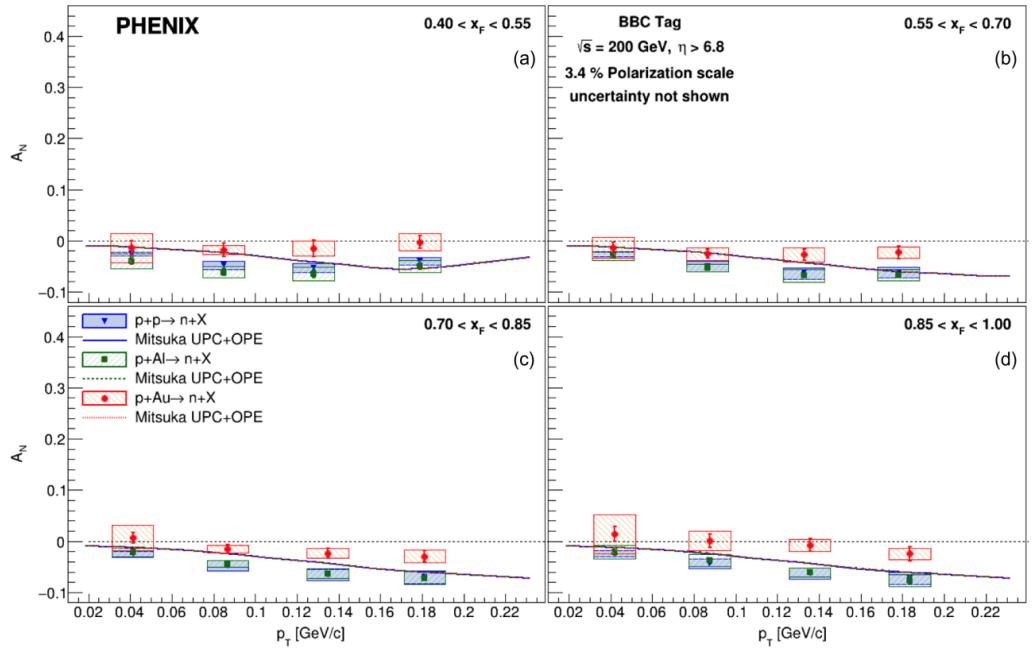


Figure 10. The p_T-dependent A_N of far-forward neutrons for $p^{\uparrow} + p$ (blue), $p^{\uparrow} + Al$ (green), $p^{\uparrow} + Au$ (red) collision systems after enhancing hadronic contributions with the BBC tag trigger condition. Comparisons to model calculations that account for contributions from one-pion exchange [58] and UPC [59] are shown at (**a**) $0.40 < x_F < 0.55$ (**b**) $0.55 < x_F < 0.70$ (**c**) $0.70 < x_F < 0.85$ (**d**) $0.85 < x_F < 1.00$.

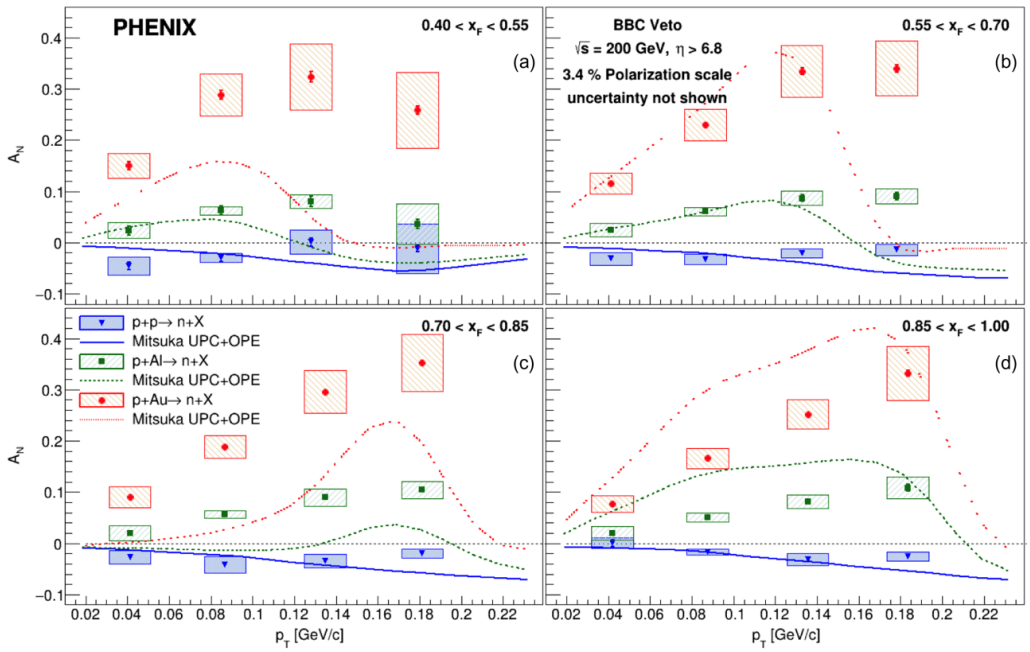


Figure 11. The p_T-dependent A_N of far-forward neutrons for $p^{\uparrow} + p$ (blue), $p^{\uparrow} + Al$ (green), $p^{\uparrow} + Au$ (red) collision systems after enhancing electromagnetic UPC contributions with the BBC veto trigger condition. Comparisons to model calculations that account for contributions from one-pion exchange [58] and UPC [59] are shown at (**a**) $0.40 < x_F < 0.55$ (**b**) $0.55 < x_F < 0.70$ (**c**) $0.70 < x_F < 0.85$ (**d**) $0.85 < x_F < 1.00$.

4. Conclusions

The PHENIX spin physics group has made a suite of recent measurements that explore the role of spin in QCD and nuclear physics. Measurements of longitudinal spin asymmetries offer evidence of nonzero gluon polarization and a positive polarized sea quark asymmetry. Measurements of transverse spin asymmetries in $p^{\uparrow} + p$ collisions constrain a wide variety of twist-3 multiparton correlators. In $p^{\uparrow} + A$ collisions, transverse spin asymmetries motivate new questions about the effects of nuclear matter in spin physics. As the PHENIX program winds down, the final spin analyses are underway. We will further explore the low-x behavior of the gluon helicity with forward measurements of longitudinal double spin asymmetries at $\sqrt{s} = 510$ GeV.

Funding: We acknowledge support from the Office of Nuclear Physics in the Office of Science of the Department of Energy, the National Science Foundation, Abilene Christian University Research Council, Research Foundation of SUNY, and Dean of the College of Arts and Sciences, Vanderbilt University (USA), Ministry of Education, Culture, Sports, Science, and Technology and the Japan Society for the Promotion of Science (Japan), Natural Science Foundation of China (People's Republic of China), Croatian Science Foundation and Ministry of Science and Education (Croatia), Ministry of Education, Youth and Sports (Czech Republic), Centre National de la Recherche Scientifique, Commissariat 'a l'Energie Atomique, and Institut' National de Physique Nucl'eaire et de Physique des Particules (France), J. Bolyai Research Scholarship, EFOP, the New National Excellence Program (UNKP), NKFIH', and OTKA (Hungary), Department of Atomic Energy and Department of Science and Technology (India), Israel Science Foundation (Israel), Basic Science Research and SRC (CENuM) Programs through NRF funded by the Ministry of Education and the Ministry of Science and ICT (Korea). Ministry of Education and Science, Russian Academy of Sciences, Federal Agency of Atomic Energy (Russia), VR and Wallenberg Foundation (Sweden), University of Zambia, the Government of the Republic of Zambia (Zambia), the U.S. Civilian Research and Development Foundation for the Independent States of the Former Soviet Union, the Hungarian American Enterprise Scholarship Fund, the US-Hungarian Fulbright Foundation, and the US-Israel Binational Science Foundation.

Data Availability Statement: The data from recent PHENIX measurements are available in HEPdata: https://www.hepdata.net/search/?collaboration=PHENIX (accessed on 7 February 2025).

Conflicts of Interest: The authors declare no conflicts of interest. The funders had no role in the design of the study; in the collection, analyses, or interpretation of data; in the writing of the manuscript; or in the decision to publish the results.

References

1. Jaffe, R.; Manohar, A. The g1 problem: Deep inelastic electron scattering and the spin of the proton. *Nucl. Phys. B* **1990**, *337*, 509–546. [CrossRef]
2. Adeva, B.; Akdogan, T.; Arik, E.; Arvidson, A.; Badelek, B.; Bardin, G.; Baum, G.; Berglund, P.; Betev, L.; Bird, I.G.; et al. Spin asymmetries A_1 and structure functions g_1 of the proton and the deuteron from polarized high energy muon scattering. *Phys. Rev. D* **1998**, *58*, 112001. [CrossRef]
3. Abe, K.; Akagi, T.; Anthony, P.L.; Antonov, R.; Arnold, R.G.; Averett, T.; Band, H.R.; Bauer, J.M.; Borel, H.; Bosted, P.E.; et al. Measurements of the proton and deuteron spin structure functions g_1 and g_2. *Phys. Rev. D* **1998**, *58*, 112003. [CrossRef]
4. Airapetian, A.; Akopov, N.; Akopov, Z.; Andrus, A.; Aschenauer, E.C.; Augustyniak, W.; Avakian, R.; Avetissian, A.; Avetissian, E.; Belostotski, S.; et al. Precise determination of the spin structure function g_1 of the proton, deuteron, and neutron. *Phys. Rev. D* **2007**, *75*, 012007. [CrossRef]
5. Prok, Y.; Bosted, P.; Kvaltine, N.; Adhikari, K.P.; Adikaram, D.; Aghasyan, M.; Amaryan, M.J.; Anderson, M.D.; Anefalos Pereira, S.; Avakian, H.; et al. Precision measurements of g_1 of the proton and of the deuteron with 6 GeV electrons. *Phys. Rev. C* **2014**, *90*, 025212. [CrossRef]
6. Adolph, C.; Akhunzyanov, R.; Alexeev, M.; Alexeev, G.; Amoroso, A.; Andrieux, V.; Anosov, V.; Austregesilo, A.; Azevedo, C.; Badełek, B.; et al. The spin structure function g1p of the proton and a test of the Bjorken sum rule. *Phys. Lett. B* **2016**, *753*, 18–28. [CrossRef]
7. Alekseev, M.; Alexakhin, V.; Alexandrov, Y.; Alexeev, G.; Amoroso, A.; Austregesilo, A.; Badełek, B.; Balestra, F.; Barth, J.; Baum, G.; et al. Quark helicity distributions from longitudinal spin asymmetries in muon–proton and muon–deuteron scattering. *Phys. Lett. B* **2010**, *693*, 227–235. [CrossRef]
8. Airapetian, A.; Akopov, N.; Akopov, Z.; Aschenauer, E.C.; Augustyniak, W.; Avakian, R.; Avetissian, A.; Belostotski, S.; Blok, H.P.; Borissov, A.; et al. Longitudinal double-spin asymmetries in semi-inclusive deep-inelastic scattering of electrons and positrons by protons and deuterons. *Phys. Rev. D* **2019**, *99*, 112001. [CrossRef]
9. Adare, A.; Afanasiev, S.; Aidala, C.; Ajitanand, N.N.; Akiba, Y.; Al-Bataineh, H.; Alexander, J.; Aoki, K.; Aphecetche, L.; Asai, J.; et al. Inclusive cross section and double helicity asymmetry for π^0 production in $p+p$ collisions at $\sqrt{s} = 62.4$ GeV. *Phys. Rev. D* **2009**, *79*, 012003. [CrossRef]
10. Adare, A.; Afanasiev, S.; Aidala, C.; Ajitanand, N.N.; Akiba, Y.; Al-Bataineh, H.; Alexander, J.; Aoki, K.; Aphecetche, L.; Asai, J.; et al. Gluon-Spin Contribution to the Proton Spin from the Double-Helicity Asymmetry in Inclusive π^0 Production in Polarized $p+p$ Collisions at $\sqrt{s} = 200$ GeV. *Phys. Rev. Lett.* **2009**, *103*, 012003. [CrossRef]
11. Adare, A.; Afanasiev, S.; Aidala, C.; Ajitanand, N.N.; Akiba, Y.; Al-Bataineh, H.; Alexander, J.; Aoki, K.; Aphecetche, L.; Armendariz, R.; et al. Cross section and double helicity asymmetry for η mesons and their comparison to π^0 production in $p+p$ collisions at $\sqrt{s} = 200$ GeV. *Phys. Rev. D* **2011**, *83*, 032001. [CrossRef]
12. Abelev, B.I.; Aggarwal, M.M.; Ahammed, Z.; Anderson, B.D.; Arkhipkin, D.; Averichev, G.S.; Bai, Y.; Balewski, J.; Barannikova, O.; Barnby, L.S.; et al. Longitudinal Double-Spin Asymmetry for Inclusive Jet Production in $\vec{p}+\vec{p}$ Collisions at $\sqrt{s} = 200$ GeV. *Phys. Rev. Lett.* **2008**, *100*, 232003. [CrossRef] [PubMed]
13. Abelev, B.I.; Aggarwal, M.M.; Ahammed, Z.; Alakhverdyants, A.V.; Anderson, B.D.; Arkhipkin, D.; Averichev, G.S.; Balewski, J.; Barannikova, O.; Barnby, L.S.; et al. Longitudinal double-spin asymmetry and cross section for inclusive neutral pion production at midrapidity in polarized proton collisions at $\sqrt{s} = 200$ GeV. *Phys. Rev. D* **2009**, *80*, 111108. [CrossRef]
14. Adamczyk, L.; Agakishiev, G.; Aggarwal, M.M.; Ahammed, Z.; Alakhverdyants, A.V.; Alekseev, I.; Alford, J.; Anderson, B.D.; Anson, C.D.; Arkhipkin, D.; et al. Longitudinal and transverse spin asymmetries for inclusive jet production at mid-rapidity in polarized $p+p$ collisions at $\sqrt{s} = 200$ GeV. *Phys. Rev. D* **2012**, *86*, 032006. [CrossRef]
15. de Florian, D.; Sassot, R.; Stratmann, M.; Vogelsang, W. Evidence for Polarization of Gluons in the Proton. *Phys. Rev. Lett.* **2014**, *113*, 012001. [CrossRef]
16. Nocera, E.R.; Ball, R.D.; Forte, S.; Ridolfi, G.; Rojo, J. A first unbiased global determination of polarized PDFs and their uncertainties. *Nucl. Phys. B* **2014**, *887*, 276–308. [CrossRef]
17. Sivers, D. Single-spin production asymmetries from the hard scattering of pointlike constituents. *Phys. Rev. D* **1990**, *41*, 83–90. [CrossRef]
18. Sivers, D. Hard-scattering scaling laws for single-spin production asymmetries. *Phys. Rev. D* **1991**, *43*, 261–263. [CrossRef]

19. Collins, J. Fragmentation of transversely polarized quarks probed in transverse momentum distributions. *Nucl. Phys. B* **1993**, *396*, 161–182. [CrossRef]
20. Airapetian, A.; Akopov, N.; Akopov, Z.; Amarian, M.; Andrus, A.; Aschenauer, E.C.; Augustyniak, W.; Avakian, R.; Avetissian, A.; Avetissian, E.; et al. Single-Spin Asymmetries in Semi-Inclusive Deep-Inelastic Scattering on a Transversely Polarized Hydrogen Target. *Phys. Rev. Lett.* **2005**, *94*, 012002. [CrossRef]
21. Alexakhin, V.Y.; Alexandrov, Y.; Alexeev, G.D.; Amoroso, A.; Badełek, B.; Balestra, F.; Ball, J.; Baum, G.; Bedfer, Y.; Berglund, P.; et al. First Measurement of the Transverse Spin Asymmetries of the Deuteron in Semi-inclusive Deep Inelastic Scattering. *Phys. Rev. Lett.* **2005**, *94*, 202002. [CrossRef] [PubMed]
22. Alekseev M.; Alexakhin V.; Alexandrov Y.; Alexeev G.; Amoroso A.; Arbuzov A.; Badełek B.; Balestra F.; Ball J.; Barth J.; et al. Collins and Sivers asymmetries for pions and kaons in muon–deuteron DIS. *Phys. Lett. B* **2009**, *673*, 127–135. [CrossRef]
23. Airapetian, A.; Akopov, N.; Akopov, Z.; Aschenauer, E.C.; Augustyniak, W.; Avetissian, A.; Avetisyan, E.; Bacchetta, A.; Ball, B.; Bianchi, N.; et al. Observation of the Naive-*T*-Odd Sivers Effect in Deep-Inelastic Scattering. *Phys. Rev. Lett.* **2009**, *103*, 152002. [CrossRef] [PubMed]
24. Ageev E.; Alexakhin V.; Alexandrov Y.; Alexeev G.; Alexeev M.; Amoroso A.; Badełek B.; Balestra F.; Ball J.; Barth J.; et al. A new measurement of the Collins and Sivers asymmetries on a transversely polarised deuteron target. *Nucl. Phys. B* **2007**, *765*, 31–70. [CrossRef]
25. Airapetian, A.; Akopov, N.; Akopov, Z.; Aschenauer, E.; Augustyniak, W.; Avakian, R.; Avetissian, A.; Avetisyan, E.; Bacchetta, A.; Belostotski, S.; et al. Effects of transversity in deep-inelastic scattering by polarized protons. *Phys. Lett. B* **2010**, *693*, 11–16. [CrossRef]
26. Adolph C.; Aghasyan M.; Akhunzyanov R.; Alexeev M.; Alexeev G.; Amoroso A.; Andrieux V.; Anfimov N.; Anosov V.; Augsten K.; et al. Sivers asymmetry extracted in SIDIS at the hard scales of the Drell-Yan process at COMPASS. *Phys. Lett. B* **2017**, *770*, 138–145. [CrossRef]
27. Seidl, R.; Grosse Perdekamp, M.; Ogawa, A.; Adachi, I.; Aihara, H.; Bahinipati, S.; Bakich, A.M.; Bartel, W.; Bitenc, U.; Bondar, A.; et al. Measurement of azimuthal asymmetries in inclusive production of hadron pairs in e^+e^- annihilation at $\sqrt{s} = 10.58$ GeV. *Phys. Rev. D* **2008**, *78*, 032011. [CrossRef]
28. Efremov, A.; Teryaev, O. QCD asymmetry and polarized hadron structure function measurement. *Phys. Lett. B* **1985**, *150*, 383–386. [CrossRef]
29. Qiu, J.; Sterman, G. Single transverse-spin asymmetries in hadronic pion production. *Phys. Rev. D* **1998**, *59*, 014004. [CrossRef]
30. Ji, X. Gluon correlations in the transversely polarized nucleon. *Phys. Lett. B* **1992**, *289*, 137–142. [CrossRef]
31. Kang, Z.B.; Qiu, J.W. Single transverse-spin asymmetry for *D*-meson production in semi-inclusive deep inelastic scattering. *Phys. Rev. D* **2008**, *78*, 034005. [CrossRef]
32. Adcox, K.; Adler, S.; Aizama, M.; Ajitanand, N.; Akiba, Y.; Akikawa, H.; Alexander, J.; Al-Jamel, A.; Allen, M.; Alley, G.; et al. PHENIX detector overview. *Nucl. Instrum. Methods Phys. Res. Sect. A* **2003**, *499*, 469–479. [CrossRef]
33. Zhou, Y.; Sato, N.; Melnitchouk, W. How well do we know the gluon polarization in the proton? *Phys. Rev. D* **2022**, *105*, 074022. [CrossRef]
34. de Florian, D.; Forte, S.; Vogelsang, W. Higgs production at RHIC and the positivity of the gluon helicity distribution. *Phys. Rev. D* **2024**, *109*, 074007. [CrossRef]
35. Abdulameer, N.J.; Acharya, U.; Adare, A.; Aidala, C.; Ajitanand, N.N.; Akiba, Y.; Akimoto, R.; Alfred, M.; Apadula, N.; Aramaki, Y.; et al. Measurement of Direct-Photon Cross Section and Double-Helicity Asymmetry at $\sqrt{s} = 510$ GeV in $\vec{p} + \vec{p}$ Collisions. *Phys. Rev. Lett.* **2023**, *130*, 251901. [CrossRef]
36. de Florian, D.; Lucero, G.A.; Sassot, R.; Stratmann, M.; Vogelsang, W. Monte Carlo sampling variant of the DSSV14 set of helicity parton densities. *Phys. Rev. D* **2019**, *100*, 114027. [CrossRef]
37. Cocuzza, C.; Melnitchouk, W.; Metz, A.; Sato, N. Polarized antimatter in the proton from a global QCD analysis. *Phys. Rev. D* **2022**, *106*, L031502. [CrossRef]
38. Acharya, U.; Adare, A.; Aidala, C.; Ajitanand, N.N.; Akiba, Y.; Akimoto, R.; Alfred, M.; Apadula, N.; Aramaki, Y.; Asano, H.; et al. Measurement of charged pion double spin asymmetries at midrapidity in longitudinally polarized $p + p$ collisions at $\sqrt{s} = 510$ GeV. *Phys. Rev. D* **2020**, *102*, 032001. [CrossRef]
39. Adare, A.; Aidala, C.; Ajitanand, N.N.; Akiba, Y.; Akimoto, R.; Al-Ta'ani, H.; Alexander, J.; Andrews, K.R.; Angerami, A.; Aoki, K.; et al. Charged-pion cross sections and double-helicity asymmetries in polarized $p + p$ collisions at $\sqrt{s} = 200$ GeV. *Phys. Rev. D* **2015**, *91*, 032001. [CrossRef]
40. Adare, A.; Aidala, C.; Ajitanand, N.N.; Akiba, Y.; Akimoto, R.; Alexander, J.; Alfred, M.; Aoki, K.; Apadula, N.; Aramaki, Y.; et al. Measurement of parity-violating spin asymmetries in $W^{\pm}$ production at midrapidity in longitudinally polarized $p + p$ collisions. *Phys. Rev. D* **2016**, *93*, 051103. [CrossRef]

41. Adare, A.; Aidala, C.; Ajitanand, N.N.; Akiba, Y.; Akimoto, R.; Alexander, J.; Alfred, M.; Aoki, K.; Apadula, N.; Aramaki, Y.; et al. Cross section and longitudinal single-spin asymmetry A_L for forward $W^{\pm} \to \mu^{\pm}\nu$ production in polarized $p+p$ collisions at $\sqrt{s} = 510$ GeV. *Phys. Rev. D* **2018**, *98*, 032007. [CrossRef]
42. Adamczyk, L.; Adkins, J.K.; Agakishiev, G.; Aggarwal, M.M.; Ahammed, Z.; Alekseev, I.; Alford, J.; Anson, C.D.; Aparin, A.; Arkhipkin, D.; et al. Measurement of Longitudinal Spin Asymmetries for Weak Boson Production in Polarized Proton-Proton Collisions at RHIC. *Phys. Rev. Lett.* **2014**, *113*, 072301. [CrossRef] [PubMed]
43. Adam, J.; Adamczyk, L.; Adams, J.R.; Adkins, J.K.; Agakishiev, G.; Aggarwal, M.M.; Ahammed, Z.; Alekseev, I.; Anderson, D.M.; Aoyama, R.; et al. Measurement of the longitudinal spin asymmetries for weak boson production in proton-proton collisions at $\sqrt{s} = 510$ GeV. *Phys. Rev. D* **2019**, *99*, 051102. [CrossRef]
44. Acharya, U.A.; Aidala, C.; Akiba, Y.; Alfred, M.; Andrieux, V.; Apadula, N.; Asano, H.; Azmoun, B.; Babintsev, V.; Bandara, N.S.; et al. Probing Gluon Spin-Momentum Correlations in Transversely Polarized Protons through Midrapidity Isolated Direct Photons in $p^{\uparrow}+p$ Collisions at $\sqrt{s} = 200$ GeV. *Phys. Rev. Lett.* **2021**, *127*, 162001. [CrossRef]
45. Kanazawa, K.; Koike, Y.; Metz, A.; Pitonyak, D. Transverse single-spin asymmetries in $p^{\uparrow}p \to \gamma X$ from quark-gluon-quark correlations in the proton. *Phys. Rev. D* **2015**, *91*, 014013. [CrossRef]
46. Koike, Y.; Yoshida, S. Probing the three-gluon correlation functions by the single spin asymmetry in $p^{\uparrow}p \to DX$. *Phys. Rev. D* **2011**, *84*, 014026. [CrossRef]
47. Adams, D.L.; Achurin, N.; Belikov, N.I.; Bravar, A.; Bystricky, J.; Corcoran, M.D.; Cossairt, J.D.; Cranshaw, J.; Derevschikov, A.A.; En'yo, H.; et al. Measurement of single spin asymmetry for direct photon production in *pp* collisions at 200-GeV/c. *Phys. Lett. B* **1995**, *345*, 569–575. [CrossRef]
48. Abdulameer, N.J.; Acharya, U.; Aidala, C.; Akiba, Y.; Alfred, M.; Andrieux, V.; Apadula, N.; Asano, H.; Azmoun, B.; Babintsev, V.; et al. Improving constraints on gluon spin-momentum correlations in transversely polarized protons via midrapidity open-heavy-flavor electrons in $p^{\uparrow}+p$ collisions at $\sqrt{s} = 200$ GeV. *Phys. Rev. D* **2023**, *107*, 052012. [CrossRef]
49. Kang, Z.B.; Qiu, J.W.; Vogelsang, W.; Yuan, F. Accessing trigluon correlations in the nucleon via the single spin asymmetry in open charm production. *Phys. Rev. D* **2008**, *78*, 114013. [CrossRef]
50. Abdulameer, N.J.; Acharya, U.; Aidala, C.; Akiba, Y.; Alfred, M.; Andrieux, V.; Apadula, N.; Asano, H.; Azmoun, B.; Babintsev, V.; et al. Transverse single-spin asymmetry of charged hadrons at forward and backward rapidity in polarized $p+p$, $p+$Al, and $p+$Au collisions at $\sqrt{s_{NN}} = 200$ GeV. *Phys. Rev. D* **2023**, *108*, 072016. [CrossRef]
51. Kanazawa, K.; Koike, Y.; Metz, A.; Pitonyak, D. Towards an explanation of transverse single-spin asymmetries in proton-proton collisions: The role of fragmentation in collinear factorization. *Phys. Rev. D* **2014**, *89*, 111501. [CrossRef]
52. Gamberg, L.; Malda, M.; Miller, J.A.; Pitonyak, D.; Prokudin, A.; Sato, N. Updated QCD global analysis of single transverse-spin asymmetries: Extracting $\tilde{H}$, and the role of the Soffer bound and lattice QCD. *Phys. Rev. D* **2022**, *106*, 034014. [CrossRef]
53. Aidala, C.; Akiba, Y.; Alfred, M.; Andrieux, V.; Apadula, N.; Asano, H.; Azmoun, B.; Babintsev, V.; Bandara, N.S.; Barish, K.N.; et al. Nuclear Dependence of the Transverse Single-Spin Asymmetry in the Production of Charged Hadrons at Forward Rapidity in Polarized $p+p$, $p+$Al, and $p+$Au Collisions at $\sqrt{s_{NN}} = 200$ GeV. *Phys. Rev. Lett.* **2019**, *123*, 122001. [CrossRef] [PubMed]
54. Miller, M.L.; Reygers, K.; Sanders, S.J.; Steinberg, P. Glauber Modeling in High-Energy Nuclear Collisions. *Annu. Rev. Nucl. Part. Sci.* **2007**, *57*, 205–243. [CrossRef]
55. Benić, S.; Hatta, Y. Single spin asymmetry in forward pA collisions: Phenomenology at RHIC. *Phys. Rev. D* **2019**, *99*, 094012. [CrossRef]
56. Gao, J.H.; Liang, Z.T.; Wang, X.N. Nuclear dependence of azimuthal asymmetry in semi-inclusive deep inelastic scattering. *Phys. Rev. C* **2010**, *81*, 065211. [CrossRef]
57. Aidala, C.; Akiba, Y.; Alfred, M.; Andrieux, V.; Aoki, K.; Apadula, N.; Asano, H.; Ayuso, C.; Azmoun, B.; Babintsev, V.; et al. Nuclear Dependence of the Transverse-Single-Spin Asymmetry for Forward Neutron Production in Polarized $p+A$ Collisions at $\sqrt{s_{NN}} = 200$ GeV. *Phys. Rev. Lett.* **2018**, *120*, 022001. [CrossRef]
58. Kopeliovich, B.Z.; Potashnikova, I.K.; Schmidt, I.; Soffer, J. Single transverse spin asymmetry of forward neutrons. *Phys. Rev. D* **2011**, *84*, 114012. [CrossRef]
59. Mitsuka, G. Recently measured large A_N for forward neutrons in $p^{\uparrow}A$ collisions at $\sqrt{s_{NN}} = 200$ GeV explained through simulations of ultraperipheral collisions and hadronic interactions. *Phys. Rev. C* **2017**, *95*, 044908. [CrossRef]
60. Acharya, U.A.; Aidala, C.; Akiba, Y.; Alfred, M.; Andrieux, V.; Apadula, N.; Asano, H.; Azmoun, B.; Babintsev, V.; Bandara, N.S.; et al. Transverse single spin asymmetries of forward neutrons in $p+p$, $p+$Al, and $p+$Au collisions at $\sqrt{s_{NN}} = 200$ GeV as a function of transverse and longitudinal momenta. *Phys. Rev. D* **2022**, *105*, 032004. [CrossRef]

Disclaimer/Publisher's Note: The statements, opinions and data contained in all publications are solely those of the individual author(s) and contributor(s) and not of MDPI and/or the editor(s). MDPI and/or the editor(s) disclaim responsibility for any injury to people or property resulting from any ideas, methods, instructions or products referred to in the content.